The International Journal of Advanced Manufacturing Technology
https://doi.org/10.1007/s00170-018-2670-x

ORIGINAL ARTICLE

Abrasive water jet drilling of advanced sustainable bio-fibre-reinforced polymer/hybrid composites: a comprehensive analysis of machining-induced damage responses

Hom Nath Dhakal[1] · Sikiru Oluwarotimi Ismail[1] · Saheed Olalekan Ojo[2] · Marco Paggi[2] · James R. Smith[3]

Received: 19 July 2018 / Accepted: 4 September 2018

Abstract
This paper aims at investigating the effects of variable traverse speeds on machining-induced damage of fibre-reinforced composites, using the abrasive water jet (AWJ) drilling. Three different types of epoxy-based composites laminates fabricated by vacuum bagging technique containing unidirectional (UD) flax, hybrid carbon-flax and carbon fibre-reinforced composite were used. The drilling parameters used were traverse speeds of 20, 40, 60 and 80 mm/min, constant water jet pressure of 300 MPa and a hole diameter of 10 mm. The results obtained depict that the traverse speed had a significant effect with respect to both surface roughness and delamination drilling-induced damage responses. Evidently, an increase in water jet traverse speed caused an increase in both damage responses of the three samples. Significantly, the CFRP composite sample recorded the lowest surface roughness damage response, followed by C-FFRP, while FFRP exhibited the highest. However, samples of FFRP and hybrid C-FFRP recorded lowest and highest delamination damage responses, respectively. The discrepancy in both damage responses, as further validated with micrographs of colour video microscopy (CVM), scanning electron microscopy (SEM) and X-ray micro-computed tomography (X-ray μCT), is attributed to the different mechanical properties of the reinforced fibres, fibre orientation/ply stacking and hybridisation of the samples.

Keywords Abrasive water jet drilling · Damage response · Traverse speed · Surface roughness · Delamination · Hybrid composite

1 Introduction

Natural fibres are an important class of reinforcing materials for developing light weight, environmentally sustainable and low-cost composites in comparison to synthetic fibre reinforcements [1]. The positive attributes of natural fibre composites (NFCs) are high specific strength and stiffness, lower production cost than synthetic fibres, reduction of wear on the machinery used to process these fibres and reduced concerns with health and safety during processing. However, NFCs have some shortcomings which include inferior mechanical properties and high moisture absorption behaviour compared to their conventional synthetic counterparts [2]. Synthetic carbon fibre-reinforced composites have several advantages that include, but are not limited to, low thermal expansion coefficients, superior rigidity, damping properties [3], mechanical and chemical durability, high strength-to-weight ratio and modulus [4]. Hybridisation between natural and synthetic fibres is a technique in which the benefits of each material can be combined to achieve a composite that demonstrates both high mechanical performance and improved environmental impact [5]. In view of the relative strengths of both natural and synthetic fibres as reinforcements, one solution to match up the mechanical properties of glass and carbon fibre composites and to enhance the water repellence behaviour of

Electronic supplementary material The online version of this article (https://doi.org/10.1007/s00170-018-2670-x) contains supplementary material, which is available to authorized users.

✉ Sikiru Oluwarotimi Ismail
sikiru.ismail@port.ac.uk

[1] School of Mechanical and Design Engineering, University of Portsmouth, Portsmouth PO1 3DJ, UK

[2] IMT School for Advanced Studies Lucca, Piazza San Francesco 19, 55100 Lucca, Italy

[3] School of Pharmacy and Biomedical Sciences, University of Portsmouth, Portsmouth PO1 2DT, UK

Published online: 15 September 2018

NFCs is hybridisation of synthetic fibres into natural fibres [6]. This approach can provide a synergic effect and gives the best properties of each of the constituent components in the resultant composites [7]. Studies carried out on hybrid composites have shown that by incorporating carbon and glass fibres into natural fibre, both mechanical and thermal properties of reinforced polymer composites were enhanced significantly [8, 9]. However, the use of NFCs in structural applications requires a thorough understanding of the influence of common manufacturing processes such as abrasive water jet (AWJ) drilling, on the overall integrity of the part. While there has been extensive studies on conventional drilling of fibre-reinforced polymer (FRP) composites [10, 12], the review of relevant literature in this paper will be limited to AWJ drilling.

Moreover, the importance of the overall quality of drilled holes, especially in heterogeneous materials such as FRP composites, is very germane. Mechanisms of creep, fatigue and wear on materials are rapidly propagated where there are high values of surface roughness and delamination responses. Poor surface roughness and inter-laminar delamination aid crack initiation and propagation as well as fibre-matrix de-bonding damage. These damages reduce the load bearing capacity, efficiency and structural integrity (durability) of the FRP composite components of systems [11]. Hence, there is need to understand these problems in terms of their mechanisms of propagation during AWJ drilling operation. This is very necessary, because of their tendency of aborting the benefits of both hybridisation and AWJ drilling techniques.

Among surface roughness, fibre pull-out/uncut, fuzzing, burr formation, thermal degradation, cracking and spalling, delamination damage has been rampantly recognised as a major problem associated with FRP composite materials drilling [13]. Unde et al. [14] reviewed the machinability of FRP composites using AWJ machining technique. They discovered that the most important process parameters were traverse speed, stand-off distance, abrasive water jet pressure and the mass flow rate. Due to the absence of heat-affected zone (HAZ) in this technique of machining of FRP composites, which is responsible for thermal distortion, they concluded that it was the most suitable method for machining the composite materials. Similarly, it has been unequivocally reported that the performance of this drilling technique significantly depended on the variation of drilling process parameters: stand-off distance, pressure [15], traverse speed, number of passes on depth of cut, angle of cutting, mass flow rate, magnitude of variation, materials machinability [16] and abrasive grit size [17]. Among these parameters, traverse speed has a great effect on the material removal rate (MRR) and surface finish of the workpiece, as surface roughness increased with an increase in traverse speed or feed rate [16, 18]. In addition, Alberdi et al. [19] reported that a significant increase in traverse feed rate caused an increase in both kerf taper angle and surface roughness. The taper angle decreased with an increasing pressure. This was attributed to the higher energy of the jet. They also found that traverse feed rate was most significant parameter affecting average surface roughness of the drilled holes.

Montesano et al. [20] adopted both conventional drilling (CD) and AWJ drilling techniques to investigate the effects of damage induced by these two techniques on the fatigue performance of a synthetic composite material (carbon fabric/epoxy plates). The experimental results obtained showed that higher surface roughness was obtained with AWJ holes when compared with the CD holes. Importantly, CD plates recorded higher stiffness degradation as well as advanced damage after a cyclic threshold. Shortly after this effect, machining-induced damage (MID) known as delamination cracks started to propagate, unlike the AWJ plates. They conclusively recommended the use of different materials systems. Hence, this supports the choice of hybrid composite in this present work. Nevertheless, Selvam et al. [21] investigated the performance of AWJ in machining (slotting) hybrid composite sample. This sample was a conventional hybrid composite laminate, comprised of both bidirectional E-glass and carbon fabrics (synthetic, not natural or sustainable fibres) with epoxy resin. They reported from their experimental results that cutting parameters such as traverse speed, abrasive mass flow rate and water pressure are important for obtaining minimum kerf taper, while traverse speed played a significant role for achieving less surface roughness.

Additionally, an investigation on the mechanics of exit-ply delamination during water jet drilling of graphite-epoxy composite laminates has been reported [22]. Using fracture mechanics and plate theory, he formulated a numerical model to optimise the water pressure needed for zero delamination effects in water jet drilling. Shaikh and Jain [23] studied the cutting mechanisms of cotton fibre polyester FRP composites, using CO_2 laser, water jet and diamond saw cutting techniques. The results obtained from their experimental analysis showed the preference of laser cutting over both water jet and diamond saw cutting, due to failure effects such as fibre pull-out in many directions during diamond saw cutting and fibre curling experienced during water jet machining of the composites. More so, the tendency of degradation of reinforced cotton fibres with moisture evidently discouraged the applicability of water jet cutting technique.

Furthermore, an experimental investigation into the micromechanical behaviour of the reinforced fibres and matrix of a unidirectional (UD) graphite-epoxy composite, using both water jet machining and abrasive water jet machining techniques, has been reported [24]. The results obtained depicted that the abrasive water jet machining produced a finer surface finish than water jet machining. This better performance was attributed to the presence of combinatory material removal mechanisms of shearing, erosion and micromachining as well as the correct choice of abrasive used

during abrasive water jet machining [17]. Thus, abrasive water jet machining was preferably considered feasible for machining FRP composites.

The reported works on AWJ machining of natural/bio-fibre-reinforced polymer composites are focused on cutting, slotting and milling, but not on experimental drilling of natural/bio-fibre-reinforced polymer and/or hybrid (with at least a bio/natural fibre) composites. Kalirasu et al. [25] reported on influence of AWJ machining (cutting) parameters on banana/polyester composite. They concluded that abrasive particle has a predominant effect on the performance of the measured output quality. Similarly, Narayanappa et al. [26] stated in their conclusion section that an increased traverse speed of water jet led to an increase in the kerf taper angle, due to a decrease in the quantity of abrasive particles penetrating during the cutting of banyan tree saw dust/polypropylene green composites. The influences of machining (slotting/cutting) parameters on MRR, kerf and surface roughness have conducted by Jani et al. [27]. They accounted that traverse speed dominantly determined the afore-mentioned drilling responses on hybrid (hemp-Kevlar/epoxy) composite and good surface quality was achieved with fillers reinforcement. In addition, Patel et al. [28] reported the importance of both traverse speed and stand-off distance during AWJ cutting of banana/unsaturated polyester composite. They concluded that increase of these parameters led to an increase in both surface roughness and kerf tapper ratio.

Based on relevant literature on AWJ drilling of composites, it can be concluded that there are no reports on a comparison between AWJ drilling of both natural and hybrid (natural and synthetic) FRP composites. Therefore, this present paper examines the influences of variable traverse speeds on AWJ drilling-induced surface roughness and delamination damage of three different advanced FRP composite samples, under constant water jet pressure and same hole diameter.

2 Materials and methods

2.1 Materials specification and fabrication

Three different types of epoxy-based FRP composite laminates samples were used for this experimental investigation, with approximated dimensions of 140 × 70 × 2 mm. HexPly® M56 epoxy was used. It was a high-performance epoxy matrix, developed for out-of-autoclave curing of composite aircraft structures. This matrix was specifically formulated for vacuum pressure cure only. Both FFRP and CFRP composite laminate samples contained SDH VTC401LV UD flax fibre and HexPly M56 UD carbon fibre prepregs, and UD carbon/flax hybrid composites, respectively, with symmetrical laminate configuration of a symmetrical ply structure of $[0/90/90/0/0/90/90/0]_s$ (Fig. 1). Each of these composite samples contained 8 plies, with 0.27 and 0.25-mm-cured ply thickness of carbon and flax fibres, respectively. Therefore, FFRP, CFRP and hybrid C-FFRP composite panels have of 2.00-, 2.16- and 2.08-mm thicknesses, respectively. The ratio of two different carbon and flax fibres used in the hybrid C-FFRP composite laminate sample was approximately 50:50. Any visible air bubbles were removed by hand. The same procedure was repeated for all the remaining plies until the panel was completed. The void content was measured to be less than 5%.

A sample aluminium-based panel was fabricated for cure cycle and hand lay operation, before the vacuum bagging technique. Vacuum consolidations were carried out after every 2 plies using the vacuum bag, a vacuum of 26 mmHg was sustained over a period of 5 min. After all the plies had been laid, a final vacuum consolidation for a duration of at least 1 h was applied. During bagging-up process, two Type K, Class 1, Tolerance ± 1.5 °C thermocouples were used per laminate to drive the oven cure cycle. Figure 2 shows the process and position of the thermocouples before bagging process. After the vacuum bag had successfully completed, the panels were cured in the curing oven, as detailed below.

The carbon fibre laminates attracted an application of – 1.00 bar full vacuum. They were ramped from 20 °C to 180 °C ± 5 °C at 1–2 °C/min., dwelled at 180 °C ± 5 °C for 60 min (with tolerance of − 5 min, + 10 min) and cooled from 180 °C to 40 °C at 0.5–5 °C/min. Similarly, the flax and hybrid flax-carbon fibres laminates attracted an application of – 1.00 bar full vacuum. They were ramped from 20 °C to 135 °C ± 5 °C at 1–2 °C/min, dwelled at 135 °C ± 5 °C for 60 min (with tolerance of − 5 min, + 10 min) and cooled from 135 °C to 40 °C at 0.5–5 °C/min. Once all the plies had been laid and the final vacuum consolidation had been completed, the laminates were covered with non-perforated release film to protect them from contaminates. The three composite samples were cut into desirable and afore-mentioned sample dimensions using the same abrasive water jet cutting process, at Fluid Profiling Ltd., Gosport, Hampshire, UK.

2.2 Experimental design and procedure

A computer numerical controlled (CNC) water jet cutting system was used to conduct the drilling experiments on all the 3 FRP samples, as depicted in Fig. 3. The sample was supported at the back with a material, called corex, before the sample was securely clamped on the machine worktable. This backup material acted as a damper by reducing the effects of jet impingement, deflection at exit region and the shock wave, induced by the high kinetic energy and pressure [15]. Based on the simple design of experiment adopted, a total of 8 holes were drilled on each of the FRP composite sample, adding up to 24 holes for the 3 different samples, using variable traverse speeds of 20, 40, 60 and 80 mm/min, constant water jet

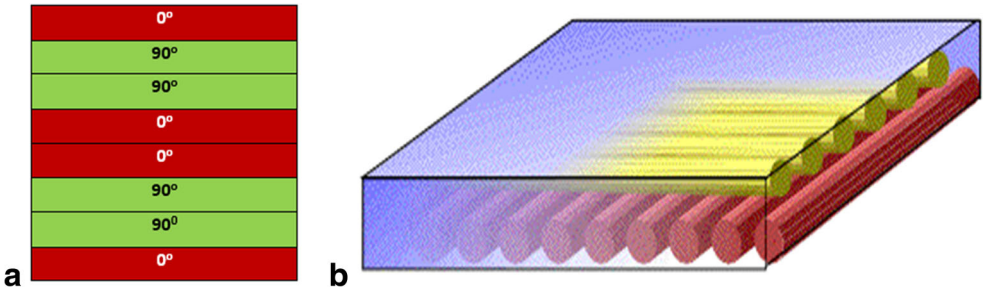

Fig. 1 Schematic illustration of the FRP composite laminate used, showing **a** laminate stacking and **b** ply orientation

pressure of 300 MPa to drill uniform hole diameter of 10 mm throughout.

2.3 Drilling conditions and mechanism

The AWJ drilling is an advanced drilling technique which employs extremely high fluid pressure to mechanically energise a jet of abrasive particles on a material surface for drilling effects, as shown in Fig. 4. Water and garnet particles were used as a cutting tool and an abrasive, respectively. A mixture of these materials produced the cutting force required for the drilling of 24 holes with a uniform diameter on the 3 different FRP composite laminate samples (8 holes per sample), under a constant abrasive water jet pressure exerted by the collimated jet.

The drilling parameters used are presented in Table 1. The abrasive particles were typically in the range of 10–80 μm in size, with flow velocity reaching as high as 80 mm/min. A nozzle of injection diameter of about 0.5 mm made up of tungsten steel, positioned at a fixed stand-off distance and a deflection angle of 60° was used to supply the pressure needed to drive the abrasive jet to the FRP composite samples. The kinetic energy developed by the abrasive particles in the transport process was then converted into a cutting force to produce the drilling effects, by erosion degradation and relative brittle fracture of the FRP composite samples. The nozzle has a range of tool life between 40 and 60 h before replacement, when its diameter has undesirably expanded due to wear and erosion. This depends on the working conditions, materials and duration.

2.4 Instrumentation

This subsection focuses on measurement of damage response. Both delamination and surface roughness were the main two damage responses considered and analysed, because they strongly affect the FRP composite parts during their service life [15]. The surface roughness or profile of the drilled holes was examined using a Mitutoyo Surftest surface profilometer with a capacity of 300.00 μm and operated by Surf software package. In addition, an overhead colour video microscope (CVM) was used for further examination and analysis of the drilled hole surface. All the 3 different samples were cut into sections (length × width × height: 8 × 2 × 4 mm, each in duplicate). The exposed half of the circumference of the drilled hole on the upper surface was separately fixed to a nickel stub using double-sided adhesive tape. The samples were illuminated with a white light source of fixed intensity and orientation with respect to the bore hole region of each sample. The illuminated samples were then viewed with an overhead colour video microscope (Sony XC-555P, Tokyo, Japan) and images captured using a USB 3.0 HD Video Capture Device (USB3HDCAP, StarTech.com, Brackmills, Northampton, UK) with integrated software (Stream Catcher). Images were quantitatively analysed by comparing red, green and blue (RGB) colour values extracted from bitmap images using an in-house program coded in Visual Basic (V6, Microsoft Inc., Redmond, WA, USA).

Similarly, a ZEISS EVO MA10 scanning electron microscope (SEM) with maximum magnification of $\times 10^5$, voltage of 15 kV and current of 50 pA was further used to examine various modes of drilling-induced damage on the drilled hole

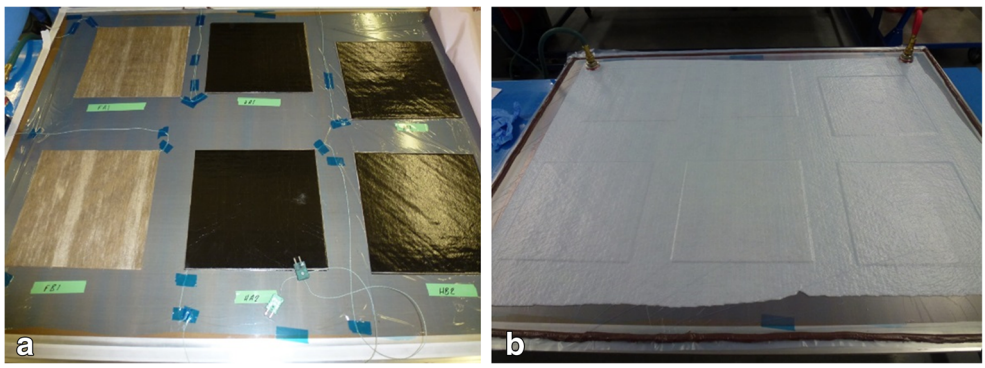

Fig. 2 Sample fabrication through vacuum consolidation, depicting process and position of the thermocouples before bagging process

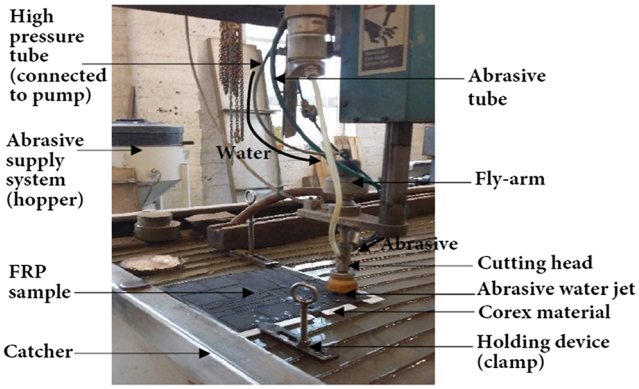

Fig. 3 The AWJ drilling experimental set-up

Table 1 AWJ drilling conditions

Parameter	Quantity
Water jet pressure (MPa)	300
Stand-off distance (mm)	4.0
Traverse speed (mm/min)	20, 40, 60, 80
Abrasive mass flow rate (kg/s)	0.003
Grit density (kg/m^3)	4100
Delay time (min)	0.05
Abrasive garnet mesh size (μm on average)	180 (80 #)
Hole diameter (mm)	10
Jet impact angle (^{o})	90

surfaces or circumferential walls. The delamination damage was observed with aid of an OLYMPUS BX 40 TH3 optical microscope (OM) with resolution and magnification of 1.0 μm and × 25 respectively and Nikon XTH 225 X-ray micro-computed tomography (X-ray μCT). The samples for each of these microscopic examinations, with exception of OM, were similarly prepared for easy examination and to properly fit on the sample stubs and probes of the instruments, as shown in Fig. 5(a, b). The micrographs obtained were thoroughly analysed and compared among the 3 FRP composite laminates, and subsequently discussed.

An arithmetic average surface roughness, R_a, was also considered throughout the measurement of surface roughness and parameters were obtained in accordance with ANSI B46.1-1978 [24]. The R_a is defined as the arithmetical average of the total perpendicular deviations of the surface profile from the contour mean line, usually determined at a particular cut-off distance [30]. Delamination occurs when a reinforced fibre plies or laminates separate under a critical compressive, tensile, bend and/or fatigue loadings, or when the threshold value is lower than the critical thrust force of drilling. Different from the conventional drilling [29], the peel-up (or entry) type of delamination damage was considered only, because it is very rampant and often greater than the push-out (or exit) delamination due to the formation of a kerf taper. Therefore, the top kerf width is greater than the bottom kerf width to form a kerf (or V) taper, as reported by Alberdi et al. [31]. The delamination damage was observed around the circumference of the drilled holes using OM measuring technique, as shown in Fig. 5(c). It was calculated by delamination extent, D_{ext}, expressed as Eq. 1 [15].

$$D_{ext} = D_{max} - D_{nom} \quad (1)$$

where D_{max} and D_{nom} (represented as D_o) are the maximum delamination damaged zone (mm) and nominal exit hole or expected diameter (10 mm), as shown in Fig. 5(c). After a trial reading, an analysis of average was performed on four different readings and taken as a process outputs for damage analysis and characterisation.

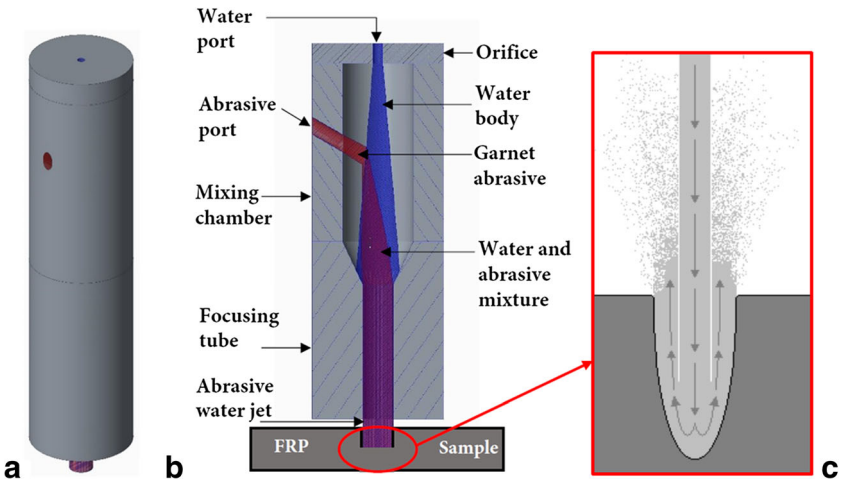

Fig. 4 (a) Schematic of a typical AWJ injection nozzle used, (b) showing its sectional features/or internal geometry and mixing of water and abrasive for (c) drilling action

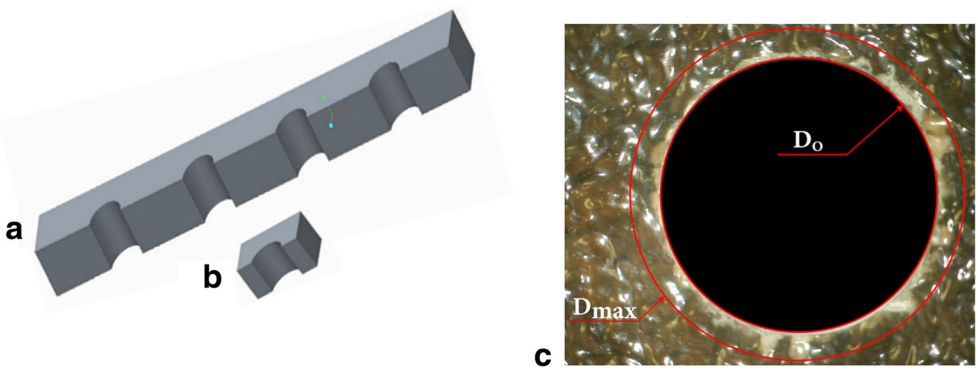

Fig. 5 Samples prepared for (a) measurement of surface roughness, (b) SEM, X-ray μCT scanner and CVM (c) analysis of delamination [29]

3 Results and discussion

3.1 Effects of traverse speed on delamination damage

The mean effects of traverse speed on delamination damage are presented in Fig. 6. It is evidently observed that the jet traverse speed greatly influenced the delamination damage on all the 3 samples considered, as the delamination damage increased with an increasing traverse speed. These results agree with that of Dhanawade and Kumar [32]. The trend of these results could be attributed to less garnet abrasive particles strike in addition to less overlapping of micro-machining process. A fewer amount of the abrasive particles reduced the primary purpose of cutting ability of AWJ, hence it caused deflection, lateral flow and increased the possibility of the water jet only developed a high thrust force that could cause an elastic deformation (delamination and uneven cut) of the entry plies. Also, delamination occurred due to the impact of the shock wave on the FRP material sample when there was no or few abrasive particles. Figure 6 shows a greatest effect of this mostly associated and critical problem (delamination) of FRP drilling on hybrid C-FFRP sample, followed by the CFRP sample. While, natural FFRP sample recorded the least delamination extent values. These experimental results are very similar with those of Ismail et al. [30], reported from their comprehensive analysis of traditional drilling of sustainable hemp fibre and conventional carbon fibre reinforced polymer composite laminate samples under a variable feed rates and cutting speeds. This damage was possibly aided by water ingress, water-wedging and abrasive particles embedment. More also, the hybridisation of the C-FFRP sample, fibres mechanical properties and ply stacking/orientation are significant contributing factors.

Furthermore, the possibility of delamination can be attributed to a low abrasive mass flow rate of 0.003 kg/s and a relatively high jet traverse speed used, especially at 60 and 80 mm/min, as recently supported by Dhanawade and Kumar [32]. The delamination defect was greater and rampant around the drilled hole entry than both at the middle and bottom or hole exit due to the elastic deformation of the first plies under a high collimated jet pressure, as exit or push-out delamination was insignificant or drastically reduced with aid of a corex backup material used.

3.2 Effects of traverse speed on surface roughness

Figure 7 shows the influence of the traverse speed on the surface roughness of the three FRP composite laminate samples. It is evident that an increase in traverse speed caused an increase in the drilled hole surface roughness of all the 3 samples, with highest surface roughness recorded in a natural FFRP composite sample, followed by the hybrid CFRP sample and the synthetic CFRP sample has the lowest surface

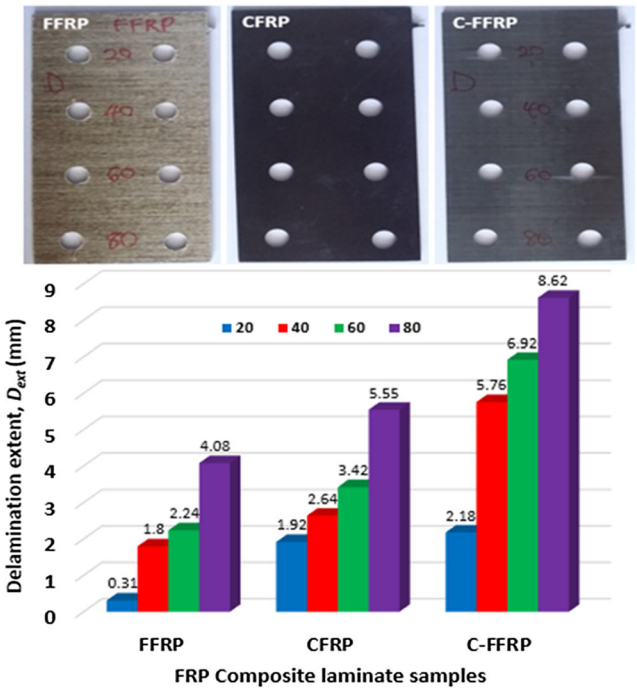

Fig. 6 The mean effects of AWJ traverse speed on delamination damage of the sample drilled holes

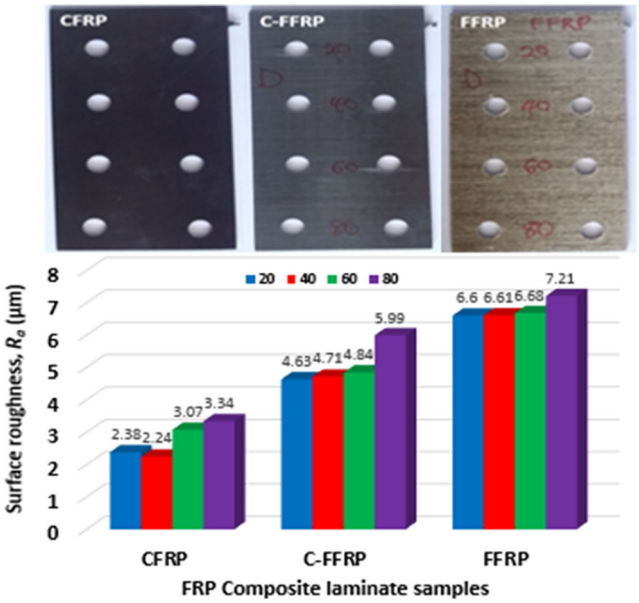

Fig. 7 The mean effects of AWJ traverse speed on surface roughness of the sample drilled holes

roughness values at different comparable traverse speeds. This infers that lower traverse speeds caused a lower surface roughness, as similarly supported by the results of machining works of Thomas [18], Fowler et al. [33] and Patel et al. [28]. But, Ojmertz [34] reported that the low traverse speeds sometimes result into uneven surface morphology and considerably increased MRR. Also, these results agree with recent experimental work reported by Ismail et al. [29], using conventional drilling technique on both natural hemp fibre-reinforced polymer (HFRP) and synthetic carbon fibre-reinforced polymer (CFRP) composite laminate samples and under a similar variable feed rates. The surface roughness of the drilled holes was greatly influenced by the jet traverse speed, as similarly and recently reported on machining of carbon/epoxy composite specimens by Hejjaji et al. [35].

In addition, a variation in the traverse speeds resulted into a significant difference in the surface roughness values recorded from the reference CFRP sample, especially between traverse speeds of 40 and 80 mm/min, when compared with other two samples with higher and similar surface roughness damage responses. This could be traced to the presence of a natural flax fibre in the other two samples. Also, it is observed that each of the flax fibre-based composite samples (FFRP and C-FFRP) has little significant surface roughness responses to an increase in traverse speeds, between 20 and 60 mm/min. The values provided are average of four readings for each type of samples. The standard deviations of the results obtained, as presented in both Figs. 6 and 7, range from ± 0.017 (minimum) to ± 0.059 (maximum) and from ± 0.024 (minimum) to ± 0.076 (maximum) for delamination and surface roughness responses, respectively.

3.3 Microscopic analysis of the drilled hole quality and other drilling-induced damage

After drilling operation, the drilled surface profiles and microstructural characteristics of the machined surfaces were examined with aids of SEM, X-ray μCT and CVM. Their micrographic results are thus analysed and discussed, respectively.

3.3.1 SEM micrographic analysis

Figure 8 depicts the different micrographs of the drilled surfaces of the 3 FRP samples, at highest traverse speed of 80 mm/min. Ramulu and Arola [24] reported in their experimental study that AWJ machining produced a finer surface finish than water jet machining due to the presence of combined material removal mechanisms of shearing, micro-machining and erosion effects of the abrasive particles as well as the correct choice of abrasive used during AWJ machining.

Also, Chen et al. [36] reported that an increase in AWJ traverse speed permitted fewer abrasives to forcibly hit on the jet target and less overlap drilling action, hence reduced the surface quality. Therefore, highest surface roughness values of 7.21, 5.99 and 3.34 μm recorded in FFRP, C-FFRP and CFRP samples respectively observed at a highest traverse speed of 80 mm/min, as evidently shown in Fig. 8, can be attributed to the presence of a much fewer garnet abrasive particles to strike the FRP sample. This is expected, because much abrasive particles are required for a finer surface finish of the samples during drilling under a combination of micro-machining, sharing, abrasion and erosion actions. Therefore, a better hole surface quality is attributed to a lower jet traverse speed.

Besides, the difference in the mechanical properties of flax and carbon fibres has contributed to the maximum delamination factors obtained with C-FFRP composite sample at same drilling conditions and parameters. Both elastic modulus and tensile strength of carbon fibres are more than that of flax fibres. The discrepancy in the properties caused a weak interfacial strength between the reinforcement (carbon/flax) and epoxy matrix. The interfacial bond between flax fibre and epoxy matrix was stronger than the interfacial bond between carbon and epoxy matrix, as both bonds (carbon-epoxy-flax) were present in the hybrid C-FFRP sample. Epoxy matrix penetrated both reinforcements (carbon and flax) differently to produce different intramolecular attractions (adhesions). The dissimilar interfacial strengths further resulted into highest delamination factor, when compared to that of carbon fibre and epoxy matrix as well as flax fibre and epoxy matrix, as present in CFRP and FFRP samples, respectively. In addition, the damage response was aided by the ply stacking and 0°–0°/90°–90° fibre orientation used when adopting hybridisation technique, which involved repetition of orientation, as previously shown in Fig. 1. It appeared that fibres of

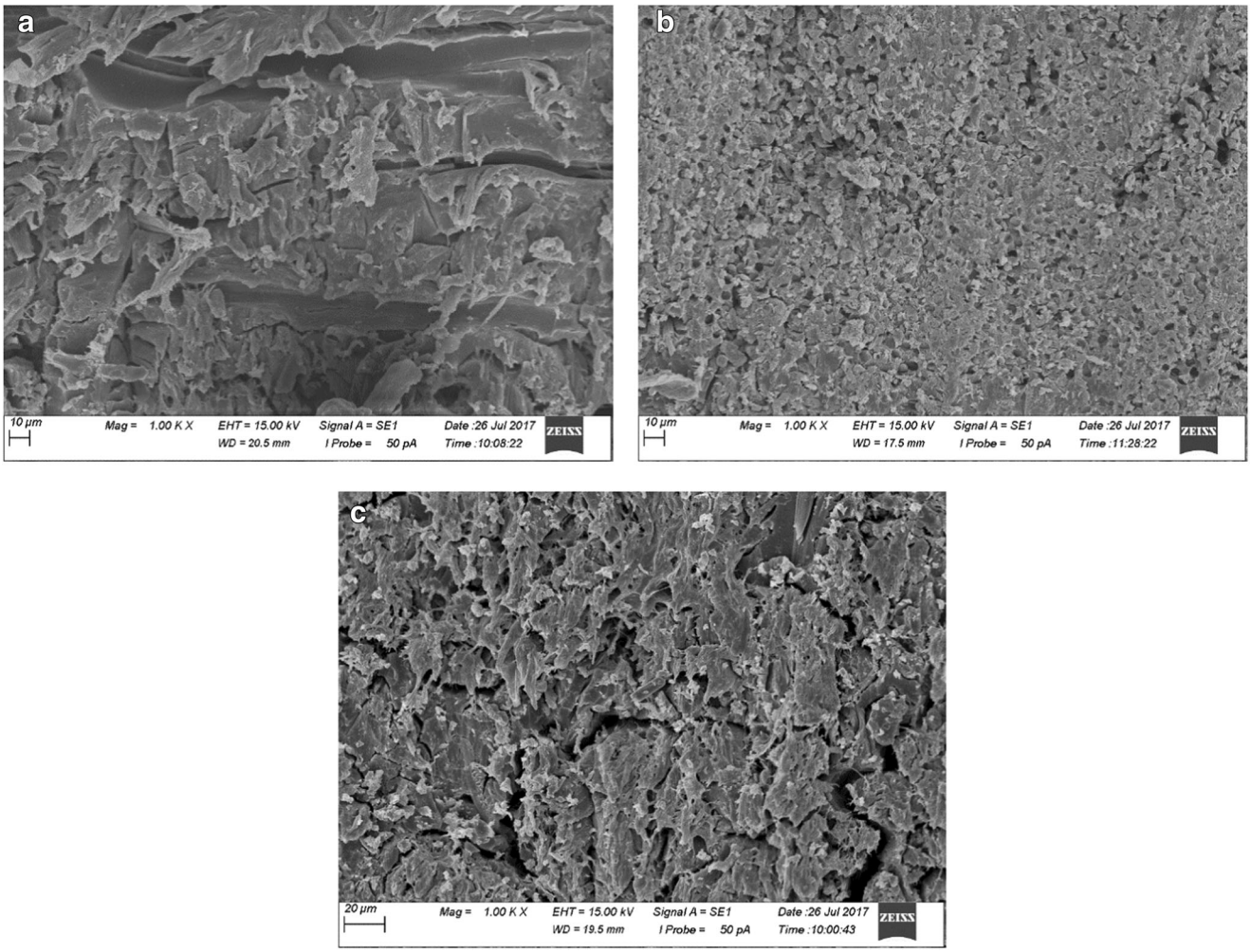

Fig. 8 Typical AWJ drilled surface SEM micrographs of **a** FFRP, **b** CFRP and **c** hybrid C-FFRP samples at highest traverse speed of 80 mm/min

same orientation were susceptible to higher delamination damage.

Also, these two fibres have different chemical reactions, interfacial bonds and compatibilities to the epoxy matrix. It is evident that FFRP composite sample exhibited best property against delamination damage. This was reflected in its lowest delamination factor, followed by the CFRP sample. The relative ductile property of flax fibre when compared to more abrasive nature of carbon fibre was enhanced with epoxy resin used. Adversely, it resulted into maximum surface roughness. The brittle materials tend to have better surface quality with lower roughness as they fracture clearly/sharply, straight, smoothly and perpendicularly, unlike ductile materials with rough fracture and resultantly, caused higher surface roughness.

Furthermore, the SEM analysis of the drilled surface texture shows the combined scooping (or sweeping) and ploughing actions, which induced a ductile shear and cutting/deformation wear phenomena of the garnet abrasive particles, respectively. These actions are very rampant with AWJ drilling technique, due to the micro-machining operation of the abrasive garnets, as stated by [37, 38]. These actions resulted into a presence of series of ridges, called striations. This was rampant with the CFRP composite sample at 80 mm/min, as shown in Fig. 9a. The common ridges effect on CFRP sample could be attributed to the abrasive nature of the carbon reinforcement. This striation effect on localised area of drilled hole surface has been similarly reported by [17, 18].

SEM micrographs further depict the presence of drilling-induced damage in form of high fractured or broken fibres and fibre-uncut or pull-out, as depicted in Fig. 9b, c. These were common at edges of the drilled holes of some FFRP composite samples, at traverse speeds of 60 and 80 mm/min. The ductile nature of the natural flax fibre reinforcement present in sample FFRP could have caused these defects. The micrographs in both Fig. 9a, b also supported the reasons behind the highest surface roughness value of 7.21 µm recorded by FFRP sample.

In addition, there were some craters or cavities in addition to cracks formed on the drilled hole walls. Cavities were caused by missing fibre segment and matrix fall-out, as shown in Fig. 9d. Among all these afore-mentioned damage, craters

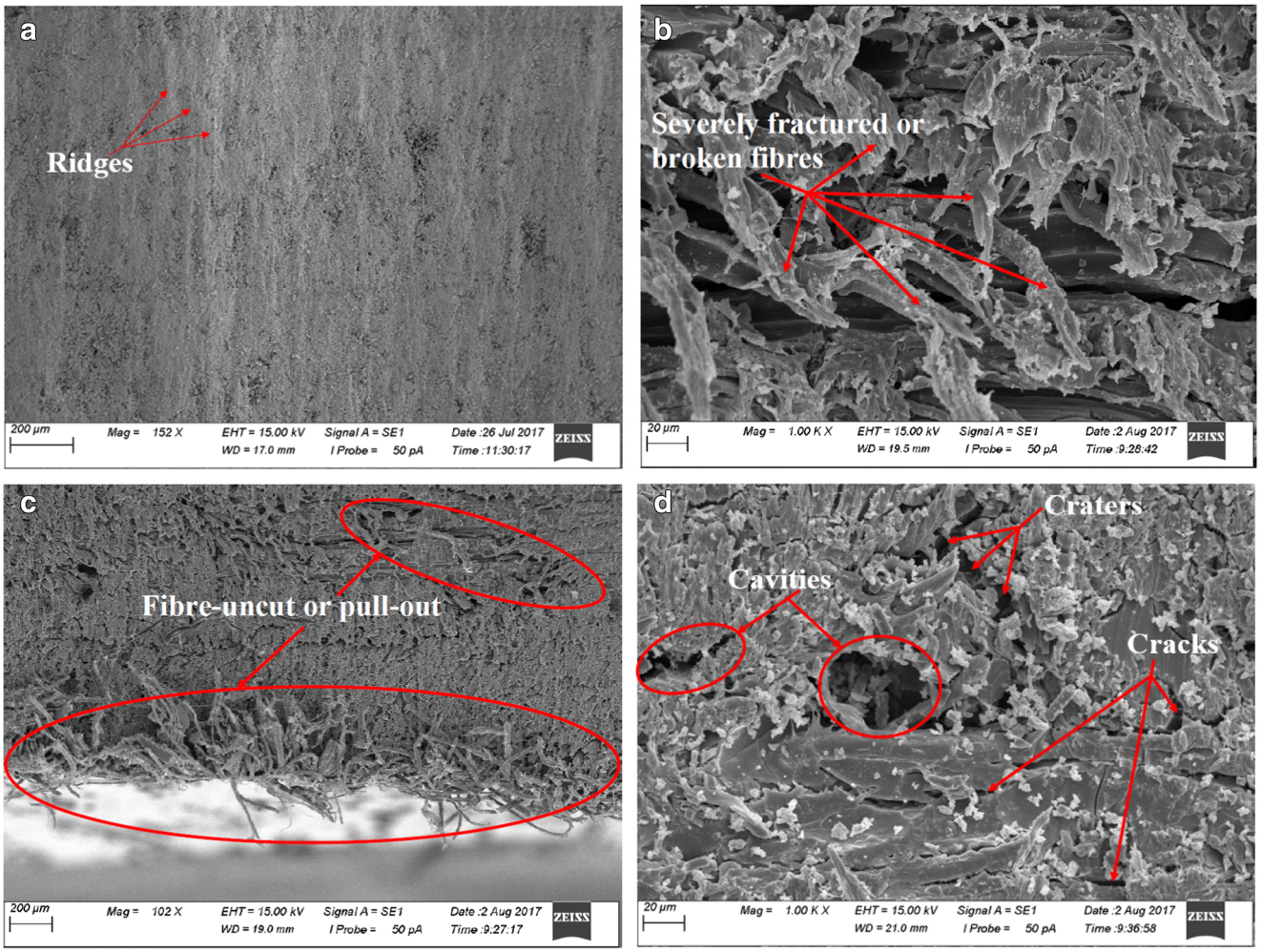

Fig. 9 Common AWJ drilling-induced damage associated with **a** CFRP at 80 mm/min, **b**, **c** FFRP at 60 mm/min and **d** C-FFRP samples at 40 mm/min

appeared to be common defect on nearly all the 3 FRP samples, with highest occurrence in the hybrid CFRP composite laminate sample. The crater diameter increased with an increasing traverse speed. Consequently, the measured surface roughness of each sample depended on the quantity and degree of broken fibres and diameters of the craters.

Lastly, the presence of garnet abrasive particles embedment was observed within an inter-laminar delamination and drilled hole walls of the hybrid C-FFRP composite laminate samples only, at all the traverse speeds used. The abrasive inclusion is depicted in Fig. 10a–d at traverse speeds of 20, 40, 60 and 80 mm/min, respectively. Figure 10a shows occurrence at the drilled hole surface while Fig. 10b–d depicts how its embedment caused inter-laminar delamination damage. These results were similarly and recently reported by Montesano et al. [20], with machining of carbon/epoxy composite specimens. Figure 10d shows the clearest micrograph of different sized embedded abrasive particles, using higher magnification. The occurrence of abrasive inclusion enhanced the propagation of inter-laminar delamination of the hybrid C-FFRP sample only, unlike other samples that have no account of abrasive inclusion. The highest delamination extent values recorded by the hybrid C-FFRP sample, as shown in Fig. 6, can be attributed to this phenomenon. This defect further embraced possibility of water ingress and water-wedging to the detriment of the structural and mechanical properties of the hybrid sample.

3.3.2 X-ray µCT images analysis

In an attempt to capture various damage locations on an entire half of the circumferential surfaces of the drilled holes which could not be effectively, clearly and easily achieved with SEM technique, the X-Ray µCT was used. Therefore, Fig. 11 depicts the micrographs of the 3 different FRP composite samples, showing their various common damage modes. The amount of stream deflection increased with an increase in traverse speed as the kinetic energy of the stream reduced, causing peel-up delamination of the plies at the hole entry. The shock wave developed by the drilling force caused an uncommon push-out delamination at exit plane due to the application of a backup plate (corex material), possibly the

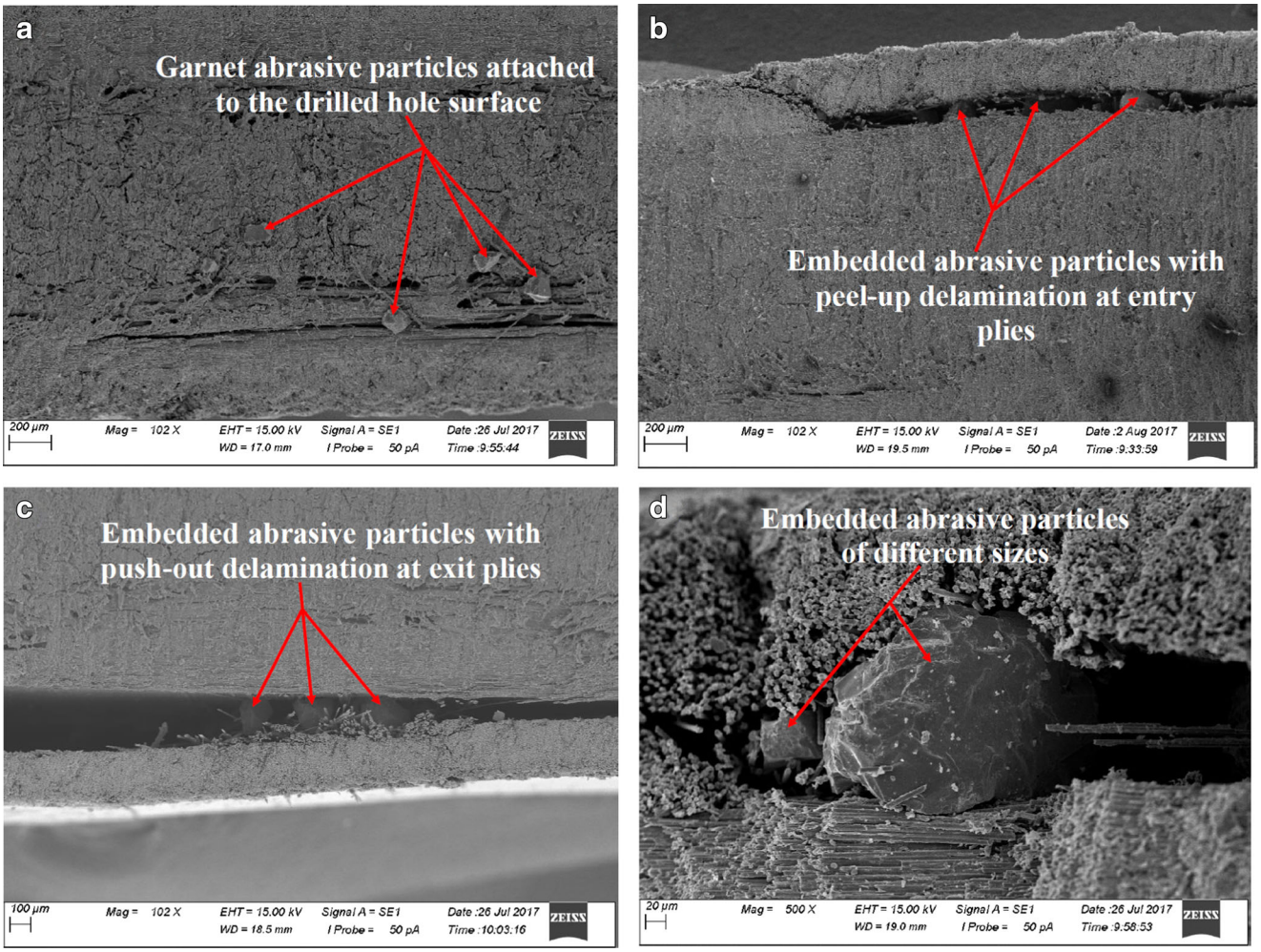

Fig. 10 Embedded garnet abrasive particles at the drilled hole wall of hybrid C-FFRP sample only when drilling at **a** 20 mm/min, caused an inter-laminar delamination, at **b** 40, **c** 60 and **d** 80 mm/min

last plies that were very close to the hole exit could not withstand this high shock wave and built-up drilling (thrust) force. These two types of delamination were scarcely observed in all the samples, with exception of a much few holes of the hybrid C-FFRP sample only, when drilling at a traverse speed of 60 mm/min (Fig. 11a). The few occurrences of these delamination MID on C-FFRP composite laminate samples have been caused by water ingress, abrasive embedment and water-wedging in the inter-laminar space aided by moderately high pressure and relatively high traverse speed of 300 MPa and 60 mm/min respectively used, in addition to the suspected weak interfacial bonds between carbon fibre and epoxy matrix as well as flax fibre and epoxy (carbon-epoxy-flax), besides hydrophobic nature of the fibres, especially in a natural flax fibre.

Figure 11b also shows the higher surface texture and roughness of the FFRP sample, comparing with the CFRP sample. These micrographic results reflect and support their statistical results earlier obtained, using surface profilometry. The scattered voids or cavities were observed at the surface of the drilled hole of CFRP samples (Figure 11c) could be probably attributed to a manufacturing defect, because it is highly impossible to have either missing carbon fibre segment or epoxy matrix fall-out due to melting and burning. Importantly, the drilling process is a cold cutting operation, without thermal stress and distortion. Otherwise, it could be drilling-induced damage caused by the drilling action of the abrasive gernet on abrasive carbon fibre of CFRP sample. The fracture (irregular breaking) of carbon fibre could have created those small voids.

3.3.3 CVM micrographic analysis

To further assess and analyse the surface nano-morphology, profile and topography (roughness) of the drilled surfaces of the 3 FRP samples, a CVM was conducted. This is necessary because both the SEM and X-Ray µCT techniques could not quantitatively show the magnitude and degree of surface roughness and for better comparison and presentation of various surface roughness responses. This innovative technique

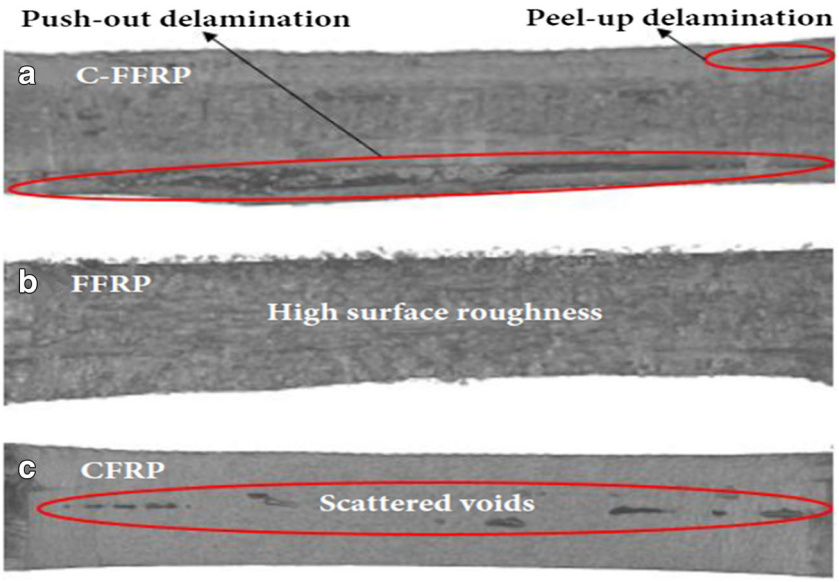

Fig. 11 X-ray μCT micrographs showing typical damage modes on the three FRP samples at a traverse speed of 60 mm/min

has been effectively used in biomedical/bio-engineering research by McGill and Mackay [39], Oha and Watanabe [40], physical science by Crocker and Grier [41] and composite technology by Hajj et al. [42]. Therefore, based on the advantages of this technique, it was adopted to investigate the surface roughness.

Figure 12 indicates that the CVM micrographs obtained at traverse speeds of 20, 40, 60 and 80 mm/min. The darker and lighter contrasts represent the lower and higher profiles of the drilled hole surface, respectively. Importantly, an increase in the jet traverse speed caused an increase in the abrasive scooping path and consequently an increase in surface roughness (most evident in the FFRP sample, Fig. 12). Moreover, the micrographs of CFRP samples appeared granular and homogenous, although no obvious change in surface texture was apparent with change in traverse speeds from 20 to 80 mm/

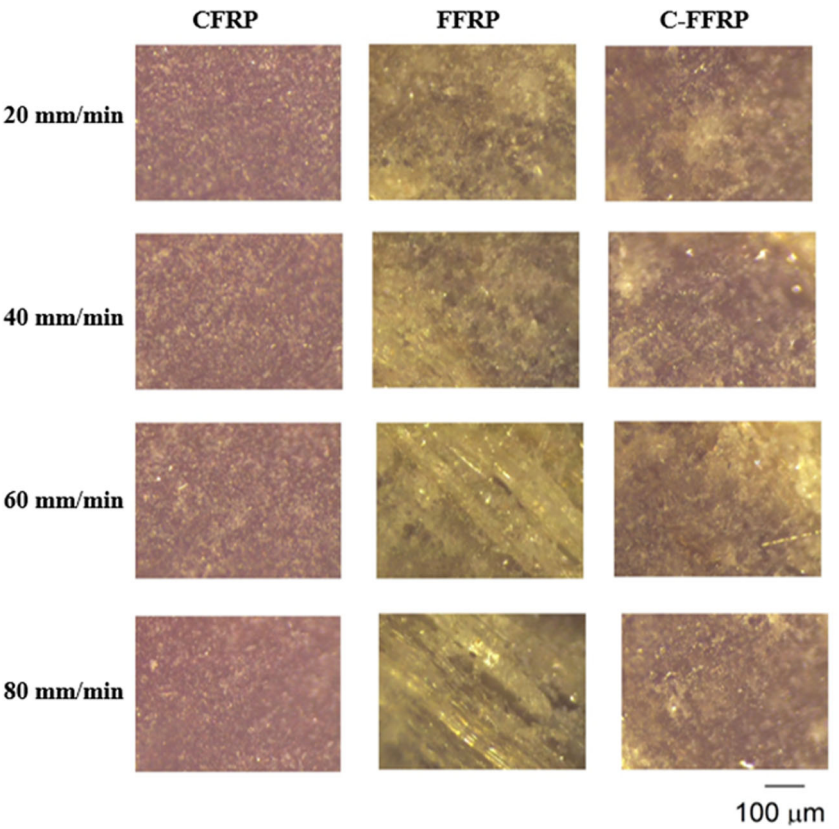

Fig. 12 CVM images of CFRP, FFRP and C-FFRP samples at AWJ traverse speeds of 20, 40, 60 and 80 mm/min; one duplicate of each shown ($n = 2$)

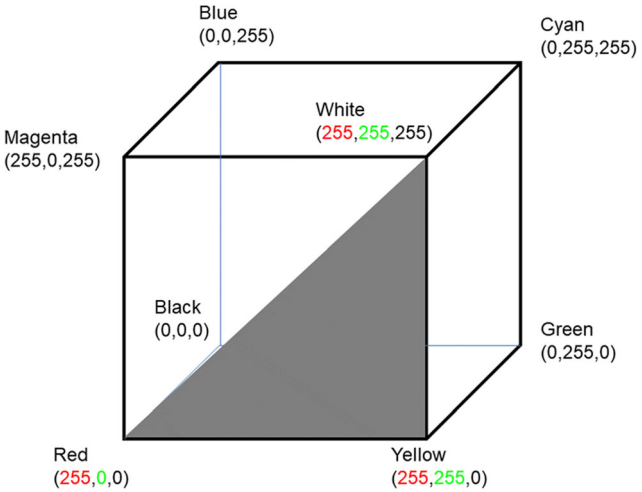

Fig. 13 Colours associated with the RGB parameter, with the grey triangle contains the red/white/yellow colours of interest and only the R + G values of sample image pixels are compared

min (Fig. 12). The FFRP sample images exhibited bundles of fibre-like features, no doubt being attributed to the flax fibres. The images seemed to indicate a progressive increase in the presence of these fibre bundles as the traverse speeds changed from 20 to 80 mm/min. More noticeable was the difference in colour of these FFRP sample images (white/yellow) in contrast to CFRP sample images (having red/pink hues). The hybrid C-FFRP sample images were a blend of the morphologies and colours exhibited by the synthetic or conventional CFRP and natural FFRP samples.

Consideration was given to the quantification of these images. The granular and fibrous appearance of CFRP and FFRP samples, respectively, was initially thought to be able to provide the quantitative approach. However, computationally, this was considered too complex relative to the much simpler method of comparing the obvious colour differences. The red vs. white/yellow comparison was assessed by comparing the bin groups of the R + G components of the RGB values for each pixel for all the sample images. R + G was chosen as a

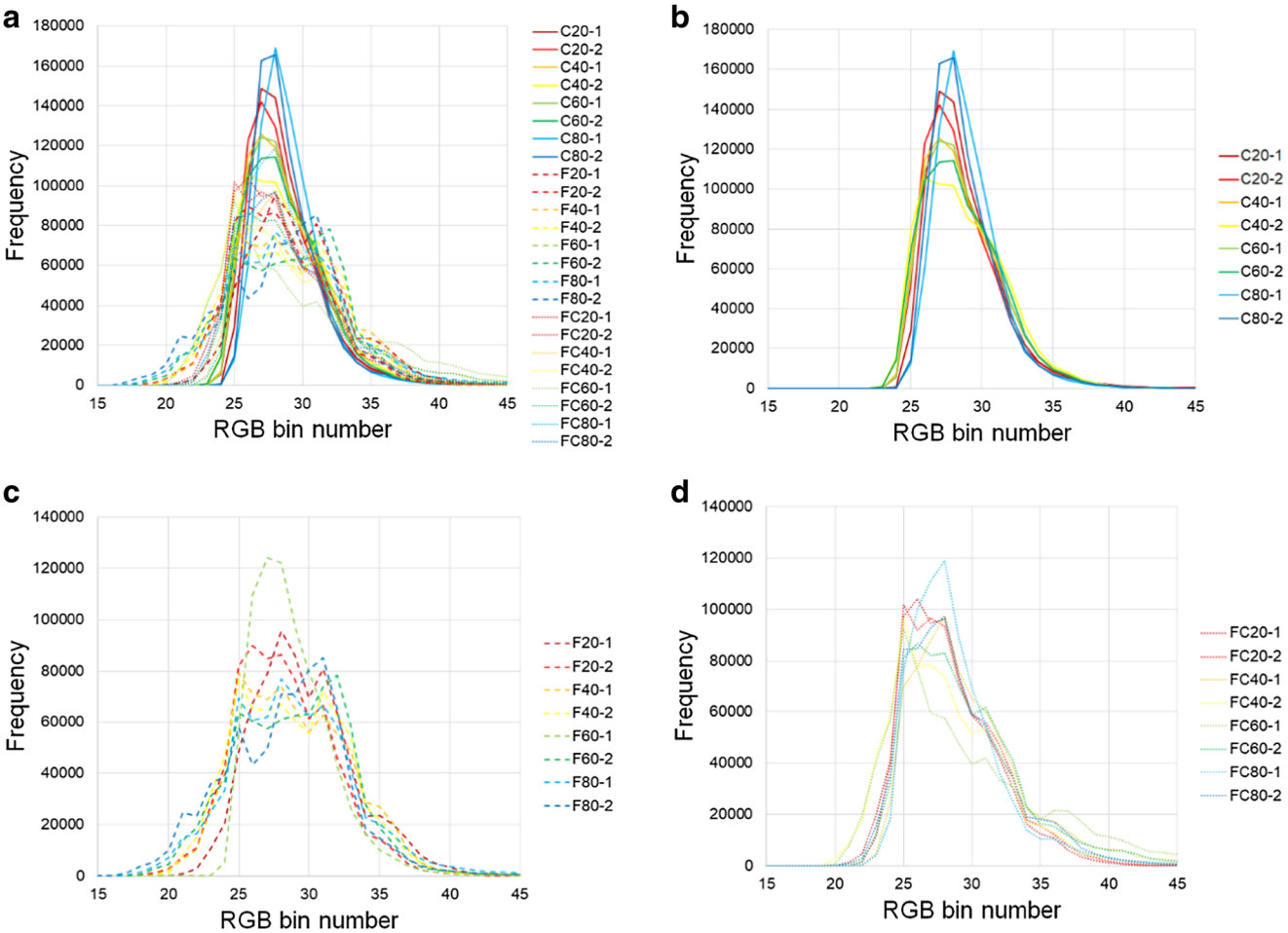

Fig. 14 Histograms of R + G bin number from RGB values of each pixel from **a** all the 3 samples (CFRP, FFRP and C-FFRP, in duplicate) from each traverse speed (20, 40, 60 and 80 mm/min); **b** as **a**, but only CFRP sample data displayed; **c** as **b** using FFRP sample data; **d** as **b** but only using C-FFRP sample data, with RGB bin number: bin 1: R + G = 0–9, bin 2: R + G = 10–19, …, bin 26: R + G = 250–259, …, bin 51: R + G = 500–510

low value for G would be expected for the CFRP sample images (predominately red, RGB = 255, 0, 0), whereas R + G should be significantly higher for white (RGB = 255, 255, 255) and yellow (RGB = 255, 255, 0) pixels, found more in the FFRP sample images (Fig. 13). The C-FFRP samples should display some intermediate value, and could potentially provide an indication of the relative mix ratios.

Histograms of the R + G bin numbers ('R + G values' henceforth) of all the samples, concentrations and duplicates are shown in Fig. 14a, with CFRP, FFRP and C-FFRP sample traces separated for convenient in Fig. 14b–d, respectively. A narrower range with necessarily higher frequency values (since image areas were the same) was found for the CFRP samples compared to FFRP and C-FFRP samples. This was expected, since the CFRP samples exhibited a red hue. Therefore, CFRP sample has a minimum value of surface roughness. This result agrees with the afore-mentioned statistical and microscopy results. A closer examination of the histogram obtained from the CFRP samples suggested that the R + G range decreased from 20 to 40 mm/min, with 60 mm/min having similar value to 40 mm/min, and then the 80 mm/min value having a higher value than the 20 mm/min samples, as shown in Fig. 14b. These results collaborate the fact that traverse speeds influence the surface roughness of the drilled hole, as earlier extensively discussed. Also, duplicate results generally backed up these observations. The reason for these differences is associated with differences in surface roughness, with deeper valleys appearing darker (more shadows). The broadest histograms were found for the FFRP sample images, reflecting the highest contribution from the G RGB component (equating to the samples being more white/yellow), as depicted in Fig. 14c. Consequently, the FFRP sample has a maximum value of surface roughness. This was most probably due to the greater heterogeneity of topography over this image area relative to that in Fig. 12. There is much obvious change in frequency or histogram width with traverse speeds found. This similarly is noticed in Fig. 7, as the FFRP sample recorded very close values of surface roughness at 20, 40 and 60 mm/min. The histograms obtained from the C-FFRP samples appeared to be a combination of those from

Table 2 Statistical data obtained from R + G bin number data from each pixel RGB value for all samples (CFRP, FFRP and C-FFRP), traverse speeds and duplicates

Sample	Median R + G value	Freq at RGB value = 28	Freq at RGB value = 23
CFRP 20-1	28	143,908	4
CFRP 20-2	28	129,450	463
CFRP 40-1	28	118,891	197
CFRP 40-2	28	101,891	1094
CFRP 60-1	28	122,097	35
CFRP 60-2	28	114,440	703
CFRP 80-1	29	169,062	2
CFRP 80-2	28	165,694	3
Mean	28	133,179 ± 24,293	313 ± 408
FFRP 20-1	29	95,472	10,643
FFRP 20-2	28	86,289	27,313
FFRP 40-1	29	73,821	26,193
FFRP 40-2	29	66,863	31,961
FFRP 60-1	31	57,781	9540
FFRP 60-2	29	61,022	31,082
FFRP 80-1	29	76,854	25,050
FFRP 80-2	29	70,816	35,869
Mean	29	73,615 ± 12,602	24,706 ± 9672
C-FFRP 20-1	28	96,096	19,955
C-FFRP 20-2	28	93,315	11,576
C-FFRP 40-1	29	97,541	5023
C-FFRP 40-2	28	73,636	42,663
C-FFRP 60-1	28	57,786	40,624
C-FFRP 60-2	29	82,843	12,543
C-FFRP 80-1	28	118,891	4046
C-FFRP 80-2	28	97,208	15,475
Mean	28	89,665 ± 18,313	18,988 ± 14,912

the CFRP and FFRP samples (Fig. 14d), as reflected in the video images presented in Fig. 12.

Lastly, the median RGB bin numbers for each trace (CFRP, FFRP and C-FFRP, every traverse speed and for both duplicates) were surprisingly close (median = 28), although the medians from the FFRP samples were very slightly higher (Table 2). The frequencies recorded for an RGB bin number of 28 (mostly at peak max) and 23 (foot of rising peak onset) provided a means to distinguish between the CFRP, FFRP and C-FFRP samples, as discussed.

4 Conclusions

The influence of the variable AWJ drilling traverse speeds has been experimentally and comprehensively investigated on both surface roughness and delamination drilling-induced damage of natural/sustainable FFRP, synthetic CFRP and hybrid C-FFRP composite laminate samples. This is a novel study for the benefit of academic research and FRP composite-based industries such as aerospace and automobile. Based on the results obtained and discussed, the following significant conclusions have been made:

- The traverse speed was a significant parameter that determined the total quality of the drilled holes. Hence, it influenced both surface roughness (profile and morphology) and delamination of the drilled holes, as both surface roughness and delamination MID of all the 3 FRP composite laminate samples decreased with a decreasing traverse speed within the selected drilling conditions considered.
- The natural UD FFRP and synthetic CFRP composite samples have a maximum and minimum surface roughness (best surface finish), respectively. This is attributed to the mechanical properties of their respective fibres. Evidently, the hybrid C-FFRP composite sample recorded the highest degree of delamination damage, followed by the CFRP sample. This is expected in the hybrid sample, because of the weak interfacial bond between the two different fibres, aided by water ingress/wedging and abrasive embedment. In addition, the effects of the different hydrophilic nature of the fibres supported the occurrence of the inter-laminar delamination.
- The SEM, X-ray μCT and CVM micrographs as well as the statistical results obtained uniformly depicted that the hybrid C-FFRP composite laminate sample recorded highest delamination MID, while FFRP samples were severely or mostly suffered from surface roughness damage, at a highest traverse speed of 80 mm/min. However, the optimal hole quality of the 3 samples was obtained at a lowest traverse speed of 20 mm/min for a minimum delamination and surface roughness MID.

Lastly, the future works will seek to consider the effects of the variable AWJ pressures, hole diameters, abrasive flow rate and stand-off distances on machining/drilling-induced damage on the same set of FRP composite laminate samples or preferably similar samples with improved mechanical properties. The comparative use of Al_2O_3 and SiC types of abrasive materials is also hereby proposed.

Acknowledgements The assistance of the following colleagues is greatly and sincerely appreciated: Mr. Joseph Dunlop and Mrs. Elaine Dyer, School of Earth and Environmental Sciences, Mr. Colin Lupton, School of Engineering, University of Portsmouth, UK.

References

1. Dhakal HN, Zhang ZY, Guthrie R, Bennett N (2013) Development of flax/carbon fibre hybrid composites for enhanced properties. J Carbo Polym 96:1–8
2. Dhakal HN, Zhang ZY, Richardson MOW (2007) Effect of water absorption on the mechanical properties of hemp fibre reinforced unsaturated polyester composites. Compos Sci Technol 67:1674–1683
3. Shyha I, Soo SL, Aspinwall D, Bradley S (2010) Effect of laminate configuration and feed rate on cutting performance when drilling holes in carbon fibre reinforced plastic composites. J Mater Process Technol 210:1023–1034
4. Irina MMW, Azmi AI, Lee CC, Mansor AF (2018) Kerf taper and delamination damage minimization of FRP hybrid composites under abrasive water-jet machining. Int J Adv Manuf Technol 94:1727–1744
5. Flynn J, Amiri A, Ulven C (2016) Hybridized carbon and flax fiber composites for tailored performance. Mater Des 102:21–29
6. Thwe MM, Liao K (2002) Effects of environmental ageing on the mechanical properties of bamboo-glass fibre reinforced polymer matrix hybrid composites. Compos Part A Appl Sci Manuf 33:43–52
7. KC B, Faruk O, Agnelli JAM, Leao AL, Tjong J, Sain M (2016) Sisal-glass fiber hybrid biocomposite: optimization of injection molding parameters using Taguchi method for reducing shrinkage. Compos Part A Appl Sci Manuf 83:152–159
8. Almansour FA, Dhakal HN, Zhang ZY (2017) Effect of water absorption on Mode I interlaminar fracture toughness of flax/basalt reinforced vinyl ester hybrid composites. Compos Struct 168:813–825
9. Nunna S, Chandra PR, Shrivastava S, Jalan A (2012) A review on mechanical behavior of natural fiber based hybrid composites. J Reinf Plast Compos 31:759–769
10. Ismail SO, Dhakal HN, Dimla E, Popov I (2017) Recent advances in twist drill design for composites machining: a critical review. Proc IMechE Part B J Eng Manuf 231:2527–2542

11. Heidarya H, Karimib NZ, Minak G (2018) Investigation on delamination and flexural properties in drilling of carbon nanotube/polymer composites. Compos Struct 201:112–120
12. Liu DF, Tang YJ, Cong WL (2012) A review of mechanical drilling for composite laminates. Compos Struct 94:1265–1279
13. Hocheng H, Tsao CC (2003) Comprehensive analysis of delamination in drilling of composite materials with various drill bits. J Mater Process Technol 140:335–339
14. Unde PD, Gayakwad MD, Ghadge RS (2014) Abrasive water jet machining of composite materials – a review. Int J Innov Res Sci Eng Technol 3:6–8
15. Phapale K, Singh R, Patil S, Singh RKP (2016) Delamination characterization and comparative assessment of delamination control techniques in abrasive water jet drilling of CFRP. Procedia Manuf 5:521–535
16. Hascalik A, Çaydaş U, G r n H (2007) Effect of traverse speed on abrasive water jet machining of Ti–6Al–4V alloy. Mater Des 28: 1953–1957
17. Thomas DJ (2009) Characteristics of abrasive waterjet cut-edges and the affect on formability and fatigue performance of high strength steels. J Manuf Process 11:97–105
18. Thomas DJ (2013) Characterisation of aggregate notch cavity formation properties on abrasive waterjet cut surfaces. J Manuf Process 15:355–363
19. Alberdi A, Artaza T, Suárez A, Rivero A, Girot F (2016) An experimental study on abrasive water jet cutting of CFRP/Ti6Al4V stacks for drilling operations. Int J Adv Manuf Technol 86:691–704
20. Montesano J, Bougherara H, Fawaz Z (2017) Influence of drilling and abrasive water jet induced damage on the performance of carbon fabric/epoxy plates with holes. Compos Struct 163:257–266
21. Selvam R, Karunamoorthy L, Arunkumar N (2017) Investigation on performance of abrasive water jet in machining hybrid composites. Mater Manuf Process 32:700–706
22. Ho-Cheng H (1990) A failure analysis of water jet drilling in composite laminate. Int J Mach Tools Manuf 30:423–429
23. Shaikh AA, Jain PS (2012) Experimental study of various technologies for cutting polymer matrix composites. Int J Adv Eng Technol 2:81–88
24. Ramulu M, Arola D (1993) Water jet and abrasive water jet cutting of unidirectional granite/epoxy composite. Compos 24:299–308
25. Kalirasu S, Rajini N, Bharath Sagar N, Mahesh KD, Gomalthi SA (2015) Studies of abrasive water jet machining (AWJM) parameters on banana/polyester composites using robust design concept. Appl Mech Mater 787:573–577
26. Ramesha N, Akhtar S, Room GT, Akhtar S (2016) Abrasive water jet machining and mechanical behavior of banyan tree saw dust powder loaded polypropylene green composites. Polym Compos 37:1754–1764
27. Jani SP, Kumar AS, Khan MA, Kumar MU (2016) Machinability of hybrid natural fiber composite with and without filler as reinforcement. Mater Manuf Process 31:1393–1399
28. Patel JK, Shaikh AA (2014) An experimental investigation of AWJ parameters on banana fiber reinforced composite. Int J Eng Res Technol 3:608–613
29. Ismail SO, Dhakal HN, Popov I, Beaugrand J (2016) Comprehensive study on machinability of sustainable and conventional fibre reinforced polymer composites. Eng Sci Technol Int J 19:2043–2052
30. Ismail SO, Dhakal HN, Dimla E, Beaugrand J, Popov I (2016) Effects of drilling parameters and aspect ratios on delamination and surface roughness of lignocellulosic HFRP composite laminates. J Appl Polym Sci 13:1–8
31. Alberdi A, Suárez A, Artaza T, Escobar-Palafox GA, Ridgway K (2013) Composite cutting with abrasive water jet. Procedia Eng 63: 421–429
32. Dhanawade A, Kumar S (2017) Experimental study of delamination and kerf geometry of carbon epoxy composite machined by abrasive water jet. J Compos Mater 0:1–18
33. Fowler G, Shipway PH, Pashby IR (2005) Abrasive water jet controlled depth milling of Ti6Al4V alloy – an investigation of the role of jet–workpiece traverse speed and abrasive grit size on the characteristics of the milled material. J Mater Process Technol 161:407–414
34. Ojmertz KMC (1993) Abrasive water jet milling: an experimental investigation. In: Hashish M (ed) Proceedings of the 7th American Water Jet Conf., water jet tech. Assoc. St. Louis, Seattle, Washington, pp 777–791
35. Hejjaji A, Zitoune R, Crouzeix L, Le Roux S, Collombet F (2017) Surface and machining induced damage characterization of abrasive water jet milled carbon/epoxy composite specimens and their impact on tensile behavior. Wear 376-377:1356–1364
36. Chen FL, Wang J, Lemma E, Siores E (2003) Striation formation mechanisms on the jet cutting surface. J Mater Process Technol 141:213–218
37. Hascalik A, Caydas U, Gurun H (2007) Effect of traverse speed on abrasive waterjet machining of Ti-6Al-4V alloy. Mater Des 28: 1953–1957
38. Seo YW, Ramulu M, Kim D (2003) Macinability of titanium alloy (Ti-6Al-4V) by abrasive waterjet. Proc Inst Mech Eng Part B J Eng Manuf 217:1709–1721
39. McGill DJ, Mackay IR (2006) The effect of ambient temperature on capillary vascular malformations. Brit J Dermatol 154:896–903
40. Oho E, Watanabe M (2001) Natural color scanning electron microscopy based on the frequency characteristics of the human visual system. Scanning 23:24–31
41. Crocker JC, Grier DG (1996) Methods of digital video microscopy for colloidal studies. J Coll Interf Sci 179:298–310
42. Hajj NE, Dheilly RM, Goullieux A, Aboura Z, Benzeggagh ML, Quéneudec M (2012) Innovant agromaterials formulated with flax shaves and proteinic binder: process and characterization. Compos Part B Eng 43:381–390